Nanoscale Conformable Coatings for Enhanced Thermal Conduction of Carbon Nanotube Films

Amy M. Marconnet[1], Munekazu Motoyama[1], Michael T. Barako[1], Yuan Gao[1], Scott Pozder[2], Burt Fowler[2], Koneru Ramakrishna[2], Glenn Mortland[2], Mehdi Asheghi[1], and Kenneth E. Goodson[1]

[1]Department of Mechanical Engineering
Stanford University,
Building 530, Room 224
440 Escondido Mall
Stanford, CA 94305
Phone: (650) 725-2086
Fax: (650) 723-7657
Email: tennocrama@gmail.com

[2]PrivaTran
1250 Capital of Texas Highway South
Building 3, Suite 400
Austin, TX 78746
Phone: (512) 680-4169
Email: rama@privatran.com

ABSTRACT

Vertically aligned carbon nanotube (CNT) arrays can provide the required combination of high thermal conductivity and mechanical compliance for thermal interface applications. Much work in the last 15 years has focused on improving the quality and intrinsic thermal conductivity of the nanotube arrays. Currently the thermal interface resistance between nanotube arrays and surrounding materials limits the overall thermal performance. To reduce this interface resistance, we propose coating the nanotube film with a continuous layer of metal. In this work, we electroplate 1 to 20 μm-thick continuous copper films directly on the carbon nanotube array. We measure the thermal conductivity of CNT arrays after electroplating using cross-sectional infrared microscopy. For low volume fraction, vertically-aligned carbon nanotubes arrays with copper electroplating (0.5 vol. %), the film thermal conductivity is nearly 3 W/m/K. These results demonstrate the feasibility of the electroplating method to coat CNT films.

KEY WORDS: thermal conductivity, carbon nanotubes, thermal interface materials,

NOMENCLATURE

A	area (m^2)
F	Faraday Constant (C/mol)
H	thickness (m)
I	current (A)
k	thermal conductivity (W/m/K)
M	molar mass (kg/mol)
n	moles of electrons per mole atoms deposited
q''	heat flux (W/m^2)
T	temperature (°C)
t	time (min)
V	voltage (V)

Greek

ρ	density (kg/m^3)

Subscripts

c	cross-sectional
Cu	of copper
e	electroplating
film	of the CNT film
i	individual CNT

INTRODUCTION

Efficient heat dissipation is critical for reliability and performance of integrated circuits, thermoelectric modules, and high power electronics. Thermal interface materials (TIMs) require low thermal resistance to transfer heat effectively and a low elastic modulus to accommodate the mismatch in thermal expansion at the interface. There is a trade-off between these two properties for conventional TIMs. Solders have low thermal resistivity but must be deposited in thick layers to avoid failing due to mechanical stresses. Greases and gels have higher thermal resistivity but can easily accommodate thermally induced stresses.

Vertically aligned arrays of carbon nanotubes (CNTs) leverage the high axial thermal conductivity of individual CNTs [1] while maintaining a low elastic modulus [2] due to the high aspect ratio and flexibility of nanotubes, making them an ideal material for TIMs. In recent years, CNT film thermal conductivity as high as solders have been reported [3]. However, the total CNT film thermal resistance, which includes both the intrinsic thermal resistivity and the thermal interface resistances between the CNT film and surrounding materials, is the key thermal metric for TIMs. The total thermal resistance can be reduced by increasing the pressure at the interface between the TIM and surrounding materials or using metal films or solders to enhance contact conductance at the interface. However, these bonding methods are challenging to adopt in a production line and do not easily accommodate variations in CNT thickness.

Here we develop a method to coat CNT films with thick metallic layers which could later be planarized using well established chemical-mechanical planarization techniques. The metal layer may enhance the thermal contact conductance between the CNT film and surrounding materials by making

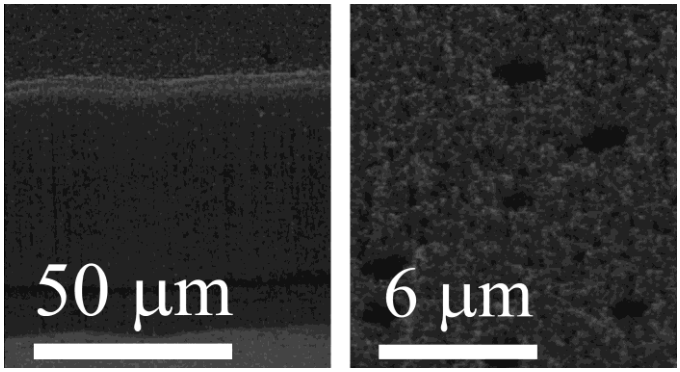

Fig. 1: SEM images of CNT film highlighting the non-uniformity in the surface of the CNT film. SEM images courtesy of Xidex Corporation.

intimate thermal contact with the CNT tips and providing a flat surface for bonding. In this work, a thin seed layer of metal (Pd and Cu) is evaporated on the top surface of the CNT film and serves as an electrode for electroplating. By varying the electroplating duration, films of copper between 1 and 20 μm are deposited uniformly on approximately 100 μm-thick CNT arrays. The thermal conductivity of metallized CNT films is measured using a steady-state cross-sectional infrared microscopy technique and the film thermal conductivity reflects the quality of the metal-CNT engagement.

FABRICATION

Five samples of ~100 μm-thick vertically aligned CNT arrays (Xidex Corp.) are electroplated with copper films. For all samples, the density of the CNT film is between 0.0105 and 0.0172 g/cm^3, corresponding to a volume fraction of approximately 0.5 vol %. As shown by the scanning electronic microscope (SEM) images in Fig. 1, the surface of the CNT array shows many defects, specifically holes in the CNT array and variations in the film thickness. Electrodeposition of a thick copper film leads to a more ideal (uniform) surface for bonding, despite the non-uniformities in the underlying CNT film.

Prior to the electroplating, a thin metal seed layer (Pd and Cu) is evaporated onto the CNT film. The Pd film enhances the adhesion of the copper to the CNTs. The copper seed layer serves an electrode for the electrodeposition process and metal

Table 1. Electroplating Conditions & Film Thickness

Sample	Seed Layer	Electroplating Time (min)	Electroplating Current (mA)	Film Thickness (μm)
A	5 nm Pd 200nm Cu	7	30	1 to 2
B	10 nm Pd 100nm Cu	40	15	4 to 6
C	10 nm Pd 100nm Cu	40	15	4 to 6
D	10 nm Pd 100nm Cu	80	15	8 to 10
E	10 nm Pd 100nm Cu	80	15	20

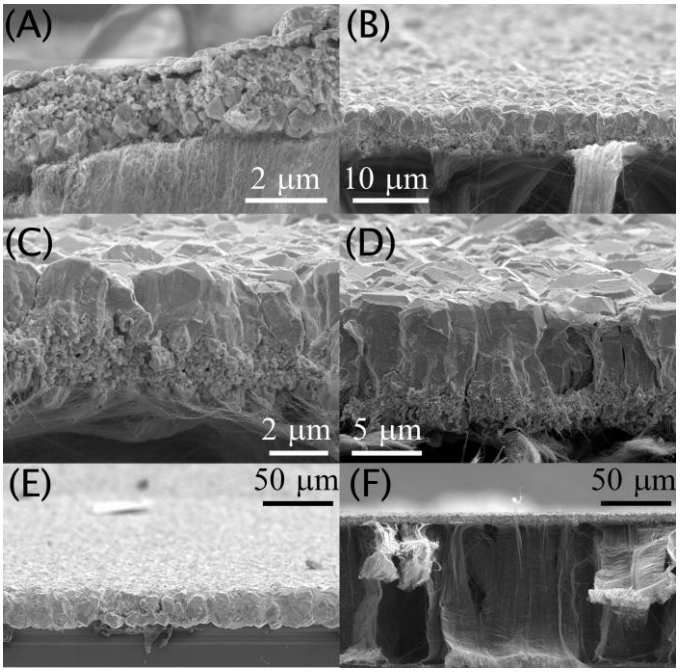

Fig. 2: Close-up SEM images of copper films on CNT arrays. Panels (A) through (E) correspond to samples A through E. Note that the image in panel E is from a region of the sample without the CNT film. (F) Zoomed-out SEM image of electroplated copper film on the CNT array (sample B) showing uniform coverage of the CNT film with copper.

lead wires are attached to the copper seed layer using silver paste cured at 100°C for ~30 minutes.

The CNT samples on their silicon growth substrate are electroplated in 2-electrode cell using a solution of $CuSO_4 \cdot 5H_2O$ and H_2SO_4. The electroplating recipe in this work is similar to that of Yang *et al.* [4], who electroplated copper to fill the space between CNTs in the arrays to form CNT-copper nanocomposites. In our method, the metal seed layer ensures that the copper layer does not deposit between the CNTs, but rather as a continuous layer on top of the CNT film. After electroplating, the samples are immediately dipped in deionized water, then ethanol, and finally dried with dry nitrogen gas.

The electroplating parameters were chosen to generate a range of film thicknesses and Table 1 shows the thickness of the seed layers, the electroplating time (t_e) and current (I_e) for each sample. Assuming the deposition is uniform across the entire area (A_e), the deposited film thickness (H_{Cu}) can be estimated by:

$$H_{Cu} = \frac{I_e t_e}{F n_{Cu}} \frac{M_{Cu}}{A_e \rho_{Cu}} \quad (1)$$

where $n_{Cu} = 2$ is the moles of electrons required for the electroplating reaction to deposit one mole of copper atoms, F is the Faraday Constant, and M_{Cu} and ρ_{Cu} are the molar mass and density of copper. The surface area for electroplating on sample A is approximately 5 cm^2, while samples B through E are approximately 2.5 cm^2. This total surface area includes a 2.5 mm wide region without CNTs near one edge of each

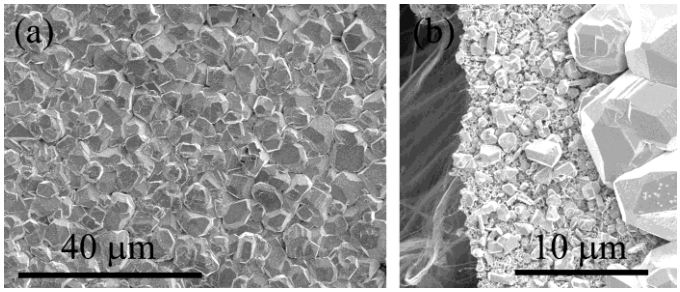

Fig. 3: SEM images of surface of copper film (sample B) near the (a) center and (b) edge of the sample. Uniform surface roughness and grain size is observed across the top surface of the sample. In panel (b), a layer of small grains is evident below the large grains at the surface.

sample.

After electroplating samples are cleaved and imaged with a SEM. The average film thicknesses determined from SEM images (see Fig. 2) are reported in Table 1. The measured thicknesses for samples A-D agree well with the expected thicknesses from Eq. (1). However, the film thickness for Sample E is much thicker than expected, possibly due to non-uniform electrodeposition. For samples A-D, the metal lead wire is attached directly to the copper seed layer on the surface of the CNT film. However, for sample E, the attachment of the metal lead wire delaminated a small portion of the copper seed layer from the CNT film. Thus, to permit electrodeposition on sample E, the lead wire is attached the sample edge without any CNTs. SEMs show electrodeposited copper on both the portions of the silicon substrate (*i.e.* the portions with and without CNTs). The film thickness reported in Table 1 for sample E is measured at a region without CNTs, near the lead attachment point and may be thicker than in other regions on the sample.

The grain structure of the copper film is evident from the SEM images. Top view SEMs (see Fig. 3) show uniform, large grains across the surface of the CNT film. Below the large grains, a layer of small grains is evident (Fig. 3(b)).

THERMAL CHARACTERIZATION

Steady state cross-sectional infrared (IR) microscopy is used to measure the thermal conductivity of the metal-coated CNT film. The copper film is used as a resistive heater to heat the top side of the CNT film, while the bottom side is attached to a temperature-controlled heat sink (see Fig. 4(a)). The square samples are cleaved into rectangles (approximately 5 mm x 15 mm) to increase the electrical resistance. Wires are attached to the edges of the copper film with silver paste. Current is passed through the copper film generating a heat flux through the CNT film and the voltage across the copper film is measured to quantify the applied heat flux:

$$q'' = \frac{IV}{A_c}. \qquad (2)$$

where I and V are the current and voltage applied to the resistive heater, A_C is the cross-sectional area of the CNT film.

Prior to measuring each sample, the IR image is calibrated by generating an emissivity map for the subsequent temperature measurements. The CNT film is brought to a uniform temperature and the calibration radiance image is

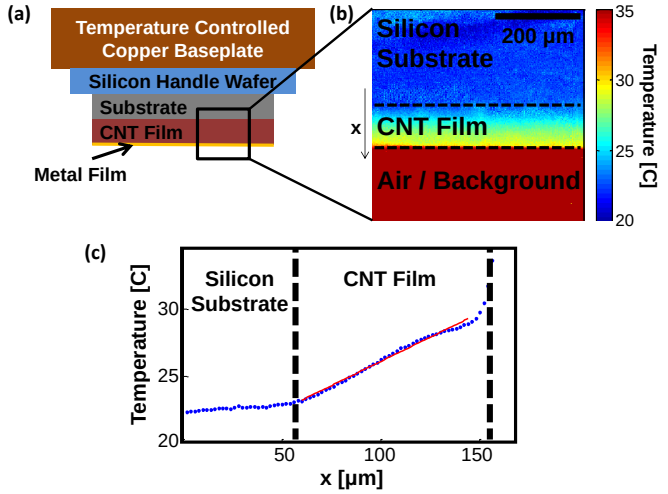

Fig. 4: Infrared Microscopy Measurement Strategy. (a) Schematic showing metalized CNT film on the silicon growth substrate attached to a secondary silicon handle wafer mounted to a temperature controlled copper baseplate. Current passed through the metal film generates a heat flux through the CNT film. (b) Two-dimensional temperature map of the CNT film during test. The temperatures are averaged for each row of pixels in the image to yield the one-dimensional temperature profile shown in panel (c). The temperature gradient in the CNT film is calculated from a least-squares linear fit (red line) to the region of the temperature profile containing the CNT film.

recorded. From this calibration image and the sample temperature (measured with thermocouples), the emissivity at each point in the sample image is determined. When the temperature is varied across the sample, the emissivity from the calibration allows measurement of the temperature from the measured radiance.

At several applied power levels (*i.e.* different heat fluxes), an infrared microscope (Quantum Focus Instruments) measures a two-dimensional (2-d) temperature map of the cross section of the CNT film (Fig. 4(b)). The temperature map is measured with a spatial resolution of 2 μm. The temperature gradient (dT/dx) within the CNT film is calculated from the 2-d temperature map by averaging the temperature in each row of pixels (*i.e.* in the direction perpendicular to the heat flux) to generate an average temperature profile (Fig. 4(c)). From Fourier's law, the thermal conductivity is extracted from the linear least squares fit to the heat flux versus temperature gradient:

$$q'' = k_{film} \frac{dT}{dx}. \qquad (3)$$

The thermal conductivity of samples B and C are 2.9 ± 0.9 W/m/K and 2.7 ± 0.8 W/m/K, respectively. As shown in Fig. 5, the thermal conductivity of the CNT films is relatively high given the low volume fraction (~0.5 vol. %) compared to other measured values for vertically aligned CNT arrays.

Reported values for the thermal conductivity of individual CNTs range from 300 W/m/K [5] to over 3000 W/m/K [1, 6-

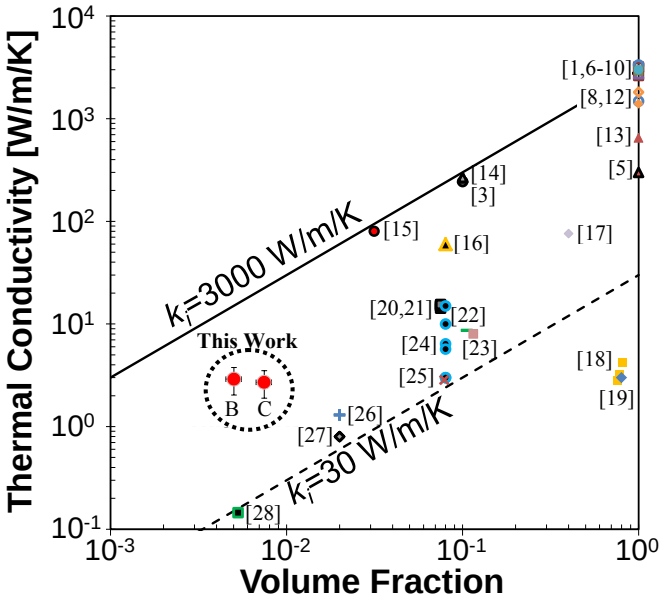

Fig. 5: Thermal conductivity as a function of volume fraction for CNT films from this work (red circles) compared to values reported for measurements for vertically-aligned CNT arrays and individual nanotubes (volume fraction = 1). The solid line shows the ideal CNT film thermal conductivity estimated for a given volume fraction using an individual nanotube conductivity of 3,000 W/m/K, while the dashed line is the estimate using an individual nanotube conductivity of 30 W/m/K.

10]. Assuming the thermal conductivity of the vertically aligned CNT films scales with the volume fraction of CNTs, the solid line in Fig. 5 shows the predicted thermal conductivity for an individual CNT thermal conductivity of k_i = 3000 W/m/K, while the dashed line assumes k_i = 30 W/m/K. These measured thermal conductivities of samples B and C correspond to effective per nanotube thermal conductivities of at least 500 W/m/K. Defects within nanotubes, CNT-CNT contacts, and poor engagement of the CNT film by the metal film all impact the measured film thermal conductivity. Given the range of reported values for individual CNTs, the electroplating process likely did not significantly damage the nanotubes. If the individual nanotubes are ideal (k = 3000 W/m/K), the measured film conductivity indicates that roughly 10% of the nanotubes physically present in the CNT array contribute to the thermal conductivity.

Since the copper film is very thin, the temperature of the metal layer cannot be resolved. Thus, the thermal boundary resistance between the metal and the CNT film cannot be determined. In future studies, the comparative cross-sectional IR method [11] will allow for more accurate determination of thermal conductivity and resolution of the boundary resistance between a reference layers and the CNT film.

CONCLUSIONS

A method for electrodepositing conformal thin films of copper on vertically aligned CNT arrays is demonstrated. The copper film is continuous and uniformly deposited across the thickness of the sample. The thermal conductivity of the CNT arrays after electrodeposition is measured to be nearly 3 W/m/K, which is comparatively high for such low density CNT films. If the copper film could be planarized, for instance with chemical mechanical planarization, this metallization layer could be used to provide a flat surface for bonding the CNT film to a heat sink. Future work to improve the thermal performance of these films can include metal deposition on higher density films and measurements of the thermal boundary resistance between the CNT and Cu film.

ACKNOWLEDGEMENTS

The authors gratefully acknowledge the support of the Air Force Research Laboratory Small Business Technology Transfer Contract FA9550-10-C-1012, the ONR (N00014-09-1-0296-P00004, Dr. Mark Spector – program manager), the NSF-DOE thermoelectrics partnership (CBET0853350), the National Science Foundation Graduate Research Fellowship program, and the Stanford Graduate Fellowship program.

References

[1] E. Pop, *et al.*, "Thermal Conductance of an Individual Single-Wall Carbon Nanotube above Room Temperature," *Nano Letters*, vol. 6, pp. 96-100, 2006.

[2] Y. Won, *et al.*, "Mechanical characterization of aligned multi-walled carbon nanotube films using microfabricated resonators," *Carbon*, vol. 50, pp. 347-355, 2012.

[3] T. Tong, *et al.*, "Dense Vertically Aligned Multiwalled Carbon Nanotube Arrays as Thermal Interface Materials," *IEEE Transactions on Components and Packaging Technologies*, vol. 30, pp. 92-100, 2007.

[4] C. Yang, *et al.*, "Carbon Nanotube/Copper Composites for Via Filling and Thermal Management," in *Proceedings of the 57th Electronic Components and Technology Conference*, 2007, pp. 1224-1229.

[5] T.-Y. Choi, *et al.*, "Measurement of the Thermal Conductivity of Individual Carbon Nanotubes by the Four-Point Three-Omega Method," *Nano Letters*, vol. 6, pp. 1589-1593, 2006.

[6] Z. Wang, *et al.*, "Length-dependent thermal conductivity of single-wall carbon nanotubes: prediction and measurements," *Nanotechnology*, vol. 18, p. 475714, 2007.

[7] Z. L. Wang, *et al.*, "Length-dependent thermal conductivity of an individual single-wall carbon nanotube," *Applied Physics Letters*, vol. 91, pp. 123119-3, 2007.

[8] Q. Li, *et al.*, "Measuring the thermal conductivity of individual carbon nanotubes by the Raman shift method," *Nanotechnology*, vol. 20, p. 145702, 2009.

[9] M. Fujii, *et al.*, "Measuring the Thermal Conductivity of a Single Carbon Nanotube," *Physical Review Letters*, vol. 95, p. 065502, 2005.

[10] P. Kim, *et al.*, "Thermal Transport Measurements of Individual Multiwalled Nanotubes," *Physical Review Letters*, vol. 87, p. 215502, 2001.

[11] A. M. Marconnet, *et al.*, "Thermal Conduction in Aligned Carbon Nanotube–Polymer Nanocomposites with High Packing Density," *ACS Nano*, vol. 5, pp. 4818-4825, 2011.

[12] C. Yu, *et al.*, "Thermal Conductance and Thermopower of an Individual Single-Wall Carbon Nanotube," *Nano Letters*, vol. 5, pp. 1842-1846, 2005.
[13] T. Y. Choi, *et al.*, "Measurement of thermal conductivity of individual multiwalled carbon nanotubes by the 3-omega method," *Applied Physics Letters*, vol. 87, pp. 013108-3, 2005.
[14] T. Tong, *et al.*, "Indium Assisted Multiwalled Carbon Nanotube Array Thermal Interface Materials," in *The Tenth Intersociety Conference on Thermal and Thermomechanical Phenomena in Electronics Systems (ITHERM '06)*, 2006, pp. 1406-1411.
[15] B. A. Cola, *et al.*, "Increased real contact in thermal interfaces: A carbon nanotube/foil material," *Applied Physics Letters*, vol. 90, pp. 093513-3, 2007.
[16] H. Xie, *et al.*, "Thermal diffusivity and conductivity of multiwalled carbon nanotube arrays," *Physics Letters A*, vol. 369, pp. 120-123, 2007.
[17] X. J. Hu, *et al.*, "3-Omega Measurements of Vertically Oriented Carbon Nanotubes on Silicon," *Journal of Heat Transfer*, vol. 128, pp. 1109-1113, 2006.
[18] H.-L. Zhang, *et al.*, "Electrical and thermal properties of carbon nanotube bulk materials: Experimental studies for the 328--958 K temperature range," *Physical Review B (Condensed Matter and Materials Physics)*, vol. 75, pp. 205407-9, 2007.
[19] H. L. Zhang, *et al.*, "Spark plasma sintering and thermal conductivity of carbon nanotube bulk materials," *Journal of Applied Physics*, vol. 97, pp. 114310-5, 2005.
[20] D. J. Yang, *et al.*, "Thermal and electrical transport in multi-walled carbon nanotubes," *Physics Letters A*, vol. 329, pp. 207-213, 2004.
[21] D. J. Yang, *et al.*, "Thermal conductivity of multiwalled carbon nanotubes," *Physical Review B*, vol. 66, p. 165440, 2002.
[22] T. Borca-Tasciuc, *et al.*, "Anisotropic thermal diffusivity of aligned multiwall carbon nanotube arrays," *Journal of Applied Physics*, vol. 98, pp. 054309-6, 2005.
[23] M. A. Panzer, *et al.*, "Thermal Properties of Metal-Coated Vertically Aligned Single-Wall Nanotube Arrays," *Journal of Heat Transfer*, vol. 130, pp. 052401-9, 2008.
[24] I. Ivanov, *et al.*, "Fast and highly anisotropic thermal transport through vertically aligned carbon nanotube arrays," *Applied Physics Letters*, vol. 89, pp. 223110-3, 2006.
[25] Y. Xu, *et al.*, "Thermal properties of carbon nanotube array used for integrated circuit cooling," *Journal of Applied Physics*, vol. 100, pp. 074302-5, 2006.
[26] Y. Son, *et al.*, "Thermal resistance of the native interface between vertically aligned multiwalled carbon nanotube arrays and their SiO_2/Si substrate," *Journal of Applied Physics*, vol. 103, pp. 024911-7, 2008.
[27] S. Pal, *et al.*, "Thermal and electrical transport along MWCNT arrays grown on Inconel substrates," *Journal of Materials Research*, vol. 23, p. 2099, 2008.
[28] X. Wang, *et al.*, "Noncontact thermal characterization of multiwall carbon nanotubes," *Journal of Applied Physics*, vol. 97, pp. 064302-5, 2005.